Proceedings of the 21st ICSMGE, Vienna, Austria, 14 – 19 June 2026. Pistrol, Adam & Schweiger (eds.)
Published by: ÖGG, Austrian Society for Geomechanics, Salzburg, Austria, ISBN 978-3-9503898-4-5
https://doi.org/10.53243/ICSMGE2026-949

Compression and shearing behavior of cement stabilized GYTTJA

Nicolas Fernandez Holdt-Olesen
Sweco, Denmark, nicolasfernandez.holdt-olesen@sweco.dk

Daniel Fernandez Holdt-Olesen
Per Aarsleff A/S, Denmark, dfho@aarsleff.com

Kenny Kataoka Sørensen
Aarhus University, Denmark, kks@cae.au.dk

Michael Lodahl
Geo, Denmark, mcl@geo.dk

ABSTRACT: Sustainable alternatives to excavation and replacement of soft organic soils are essential for reducing CO_2 emissions and resource consumption in infrastructure projects. While cement stabilization has shown promise for improving soft clay properties, the fundamental compression and yielding mechanisms of stabilized organic soils under complex stress conditions remain poorly understood, limiting the development of reliable constitutive models. This paper presents a comprehensive experimental investigation of cement stabilized gyttja behavior through triaxial stress path tests and Constant Rate of Strain consolidation tests. The study focuses on marine, postglacial, soft organic clayey silty gyttja stabilized with a cement content of 75 kg/m³ cured for 28 days at 22°C. Key findings demonstrate that cementation transforms the material from normally consolidated to an apparent overconsolidated state, introducing yield stresses unrelated to natural stress history. The material exhibits distinct pre-yield and post-yield behavior: specimens consolidated below yield show tension cut-off governed failure with dilative tendencies, while post-yield specimens display brittle behavior with significant softening. All specimens fail along single shear planes, with undrained tests showing more brittle response compared to drained tests. Effective strength parameters reveal a clear transition from peak cementation-controlled behavior ($\phi'_{\mathrm{p}} = 34.8°$, $c'_{\mathrm{p}} = 137$ kPa) to final-state frictional resistance ($\phi'_{\mathrm{fs}} = 30.3°$, $c'_{\mathrm{fs}} = 57$ kPa), with final points converging toward a limiting stress state. The results provide essential parameters for constitutive modelling and demonstrate the viability of cement stabilization as a sustainable ground improvement technique for organic soils.

KEYWORDS: Cement stabilization, organic soils, yielding, compression and shearing behavior, triaxial testing.

1 INTRODUCTION

Soft organic soil deposits such as gyttja, which are prevalent in many parts of Denmark, present significant challenges for infrastructure development and are a particular problem for harbor developments. Obtaining disposal at sea permits for dredged materials involves strict requirements, which further complicates these projects. Furthermore, traditional excavation and replacement approaches generate substantial CO_2 emissions and consume scarce resources (Larsen et al., 2019). Cement stabilization offers a sustainable alternative by improving soil properties through hydration and pozzolanic reactions (Janz and Johansson, 2002). However, the fundamental mechanical behavior of stabilized organic soils under complex stress conditions remains poorly understood, limiting reliable constitutive model development and hindering confident implementation of sustainable ground improvement practices.

Existing research has focused primarily on strength development and basic properties, leaving critical aspects inadequately addressed. The evolution of yield surfaces under isotropic and anisotropic stress conditions, stress-path dependent behavior across pre- and post-yield regimes, and the applicability of critical state frameworks to cemented organic soils require systematic investigation. While cement addition transforms soil from normally consolidated to an apparent overconsolidated state (Lee et al., 2004; Åhnberg, 2006), the specific mechanisms governing this behavior in organic soils remain unclear. Although previous work links the behavior of cement stabilized soft clay to the critical state framework and has explored aspects such as structure and yield surface evolution (Lee et al., 2004; Kasama et al., 2000), the existing studies remain limited, and a more comprehensive understanding of compression, yielding, and shearing mechanisms under varied stress paths is still needed to advance constitutive modelling and support reliable engineering design.

In this paper, selected laboratory test data is presented from an in-depth study focusing on the compression and shearing behavior of cement stabilized gyttja (cf. Holdt-Olesen et al., 2024). The material behavior is examined through a series of triaxial stress path tests and Constant Rate of Strain (CRS) consolidation tests conducted on cement stabilized gyttja with a cement content of 75 kg/m^3 cured for 28 days at a curing temperature of 22°C. The performed tests are not intended for direct practical application. The focus is on characterizing the material response under various stress and loading conditions, including stress levels significantly exceeding those typically encountered in practice. The results obtained for the cement stabilized gyttja in this study are expected to be applicable to other cement stabilized organic clayey soft soils.

2 TESTING MATERIAL AND TEST METHODS

2.1 *Testing material*

The natural soil used for the laboratory tests in this study is a marine, postglacial, soft, organic, clayey, silty gyttja, which was extracted at a depth of 2 m from Aarhus University's soft soil test site situated at Randers Harbor, Denmark (UTM32E89 X: 565577 (m) Y: 6257802 (m)). The soil contains numerous shells and shell fragments and has grey color with a greenish tint, as seen in Figure 1. The determined classification parameters for the natural gyttja are presented in Table 1, where c_{fv} and c_{u} were determined by Brandt et al. (2025).

The natural water content is slightly higher than the liquid limit. The liquid limit (fall cone method) and plastic limit were determined in accordance with DS/EN ISO 17892-12:2018.

The organic content was measured by loss on ignition (LOI), and the particle size distribution was determined through a combination of hydrometer analysis and dry sieving.

Table 1. Soil classification parameters.

Parameter	Symbol	Value (average)	Unit
Unit weight	γ	15	[kN/m^3]
Water content	w	105-115 (109)	[%]
Plastic limit	w_P	42-48 (45)	[%]
Liquid limit	w_L	97-107 (102)	[%]
Plasticity index	I_P	55-59 (57)	[%]
Organic content	LOI	7.1-8.4 (7.7)	[%]
Eff. friction angle	ϕ'	33.6	[°]
Eff. cohesion	c'	7.2	[kPa]
Field vane strength	c_{fv}	20	[kPa]
Undr. shear strength (plate load test)	c_u	12	[kPa]
Clay fraction	-	38.3	[%]
Silt fraction	-	57.5	[%]
Sand and gravel fraction	-	4.2	[%]

Figure 1. Left: natural gyttja; right: cement stabilized specimen.

2.2 *Specimen preparation*

For the triaxial tests performed in this study, cylindrical specimens with the dimensions 100 x 50 mm (H/D = 2) were used. The specimen preparation procedure followed the guidelines outlined by Helle et al. (2021), with all specimens prepared at the natural moisture content of the gyttja. Significant shell fragments were removed prior to sample preparation.

The natural gyttja was homogenized and remolded by stirring it in a mixer for 2 × 30 seconds. The cement was added as dry powder, and the mixing procedure of 2 × 30 seconds was then repeated. The cement used in this project is an ordinary Portland cement called FUTURECEM cement from Aalborg Portland A/S. The cement stabilized gyttja investigated in this study has a cement content of 75 kg/m^3 with respect to the bulk wet volume of the gyttja. The stabilized soil was manually compacted into acrylic cylindrical molds using a wooden muddler in 6 layers of the same height, and each layer was scored to ensure bonding between the layers. During curing, each specimen was placed inside two sealed plastic bags, with a damp cloth on top, to ensure 100% relative humidity and to prevent the samples from drying out. All specimens were cured at room temperature corresponding to 22°C for 28 days. The selected cement content was considered a feasible compromise between reducing the CO_2 footprint and achieving a significant strength gain (Holdt-Olesen et al., 2025; Tanderup, 2023). The curing conditions and duration were chosen to limit further strength development during testing by minimizing additional curing effects. The expected strength gain under field-temperature conditions can be estimated using the equivalent curing time approach proposed by Åhnberg and Holm (1987). The relative humidity and curing temperature were monitored and verified using Tinytag Plus 2 data loggers.

The quality and uniformity of the compacted specimens were controlled by measuring the weight of each specimen. A maximum weight deviation of 3.2% was observed, which confirms the chosen compaction method's consistency and reliability. All specimens were also visually inspected prior to testing, with attention given to identifying voids and defects that could potentially influence the results; however, due to the compaction method in a cylindrical mold, all samples were highly uniform with no edge defects or significant voids (see example of cement stabilized specimen in Figure 1).

2.3 *Test methods and experimental program*

In this study, several types of triaxial tests were performed, including isotropically consolidated undrained (CIU) tests, anisotropically consolidated undrained (CAU) tests, isotropically consolidated drained (CID) tests, and anisotropically consolidated drained (CAD) tests. A total of 17 consolidated triaxial tests were conducted on the cement stabilized gyttja, of which four were not sheared. The specimens were consolidated to either a pre-yield state (A) or a post-yield state (B), after which drained shearing (D) or undrained shearing (UD) was performed.

The consolidated triaxial tests were performed using load-frame–based automated triaxial systems equipped with stepper-motor-controlled cell pressure and back-pressure actuators. Pore pressure was measured using an independent pressure transducer installed on the base drainage line in close proximity to the specimen. The triaxial specimens were saturated by simultaneously increasing the cell pressure to 780 kPa and the back pressure to 760 kPa while maintaining an effective stress of 20 kPa. The pressures were raised over 2 hours and then held constant for 18 hours to ensure full saturation. Saturation of the specimens was verified by measuring Skempton's B-value for three cell pressure increments of 50 kPa, and all tests reached B-values above 0.95, which was chosen as the criterion for full saturation of the specimens.

A stress rate of 0.5 kPa/min was applied during consolidation stages, while the applied axial deformation rate in shearing was generally 0.004 and 0.008 mm/min for drained and undrained shearing respectively. The selected shearing rates were estimated conservatively based on observed consolidation behavior to ensure stable pore pressure responses without significant gradients across the specimen (undrained) or full dissipation of pore water pressures throughout shearing (drained). A few tests were run at slightly different rates during shearing; however, this was assessed to have insignificant influence on the results. Side drains were applied in all triaxial tests to accelerate consolidation and reduce test duration, using DuPont Typar SF40 geotextile.

Figure 2 provides an overview of the triaxial stress paths in $p' - q$ space, illustrating the consolidation states and the subsequent shearing phases. The slope of the consolidation stress paths, m, is defined based on the coefficient of lateral earth pressure, K.

$$m = \frac{\Delta q}{\Delta p'} = \frac{3(1-K)}{1+2K} \tag{1}$$

Where $K = \sigma'_h/\sigma'_v$ describes the ratio between the horizonal effective stress, σ'_h, and the vertical effective stress, σ'_v. The cross-sectional area of the specimens during the triaxial tests was calculated using a uniform cross-sectional area correction in accordance with DS/EN ISO 17892-9:2018.

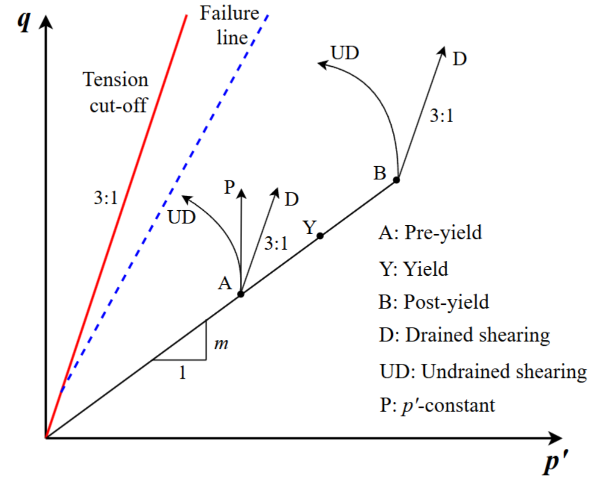

Figure 2. Triaxial test overview.

In addition to the triaxial tests performed, a total of six Constant Rate of Strain (CRS) consolidation tests were performed (in accordance with ASTM D4186-89R98) in this study to investigate the compression behavior and derive consolidation parameters for the cement stabilized gyttja.

3 RESULTS

Table 2 summarizes the triaxial test conditions and state variables. Here p'_c, q_c, and e_c denote the mean effective stress, deviatoric stress, and void ratio at the end of consolidation, while p'_y denotes the yield point, q'_{max} is the peak deviatoric stress, and $\varepsilon_{q.f}$ is the deviatoric strain at failure. Tests are grouped by pre- or post-yield consolidation state.

Table 2. Triaxial tests states and results.

ID	Consolidation K [-]	p'_c [kPa]	q_c [kPa]	e_c [-]	p'_y [kPa]	Shear q'_{max} [kPa]	$\varepsilon_{q.f}$ [%]
Consolidation to pre-yield state:							
26	1	60	0	2.56	-	486[U]	12.2
50	1	385	0	2.09	-	577[U]	1.5
9	0.5	197	148	2.43	-	532[P]	2.0
21	0.5	199	149	2.39	-	895[D]	7.3
11	0.4	222	218	2.35	-	522[U]	6.0
Consolidation to post-yield state:							
4	1	2082	0	1.65	785	6020[D]	19.6
27	1	2078	0	1.77	753	1691[U]	3.5
30	1	1486	0	1.62	580	1391[U]	2.5
62	0.7	1174	443	-	625	-	
66	0.7	1946	734	-	640	-	
20	0.5	1522	1194	1.76	540	3555[D]	15.6
24	0.5	1492	1124	1.81	568	1640[U]	1.6
28	0.5	1495	1123	1.82	570	3323[D]	15.5
8	0.5	2763	2051	1.46	608	2763[U]	1.8
17	0.4	1240	1271	1.85	458	1499[U]	1.2
70*	0.38	1795	2038	-	490	-	
65*	0.38	1834	2143	-	505	-	

[U] Undrained shearing, [D] Drained shearing, [P] Constant p' shearing
* Automatic K_0

Table 3. Compression and effective strength parameters.

Parameter	Symbol	Value (average)	Unit
Coeff. earth pressure	K_0	0.38	[-]
Gradient – NCL	λ	0.508-0.781 (0.610)	[-]
Gradient – swelling	κ	0.025-0.037 (0.030)	[-]
Friction angle – peak	ϕ'_p	34.8	[°]
Eff. cohesion – peak	c'_p	137	[kPa]
Fr. angle – final state	ϕ'_{fs}	30.3	[°]
Eff. coh. – final state	c'_{fs}	57	[kPa]

3.1 *Volumetric compression and yielding under isotropic and anisotropic conditions*

An overconsolidated state and gradual yielding were observed in all consolidated stress paths reaching high stress levels, as well as in CRS tests on the cement stabilized gyttja.

Figure 3 presents compression curves from both triaxial tests (isotropic and anisotropic consolidation) and a CRS one-dimensional consolidation test, showing void ratio, e, as a function of mean effective stress, p', on a semi-logarithmic scale. The mean effective stress in the CRS consolidation test was calculated using the at-rest earth pressure coefficient, K_0, which is determined to be 0.38 from two automatic K_0-triaxial tests (ID 70 and ID 65), as shown in Table 3. The automatic K_0-triaxial tests were performed to keep a constant diameter of the specimen based on measurement of back volume and axial displacement.

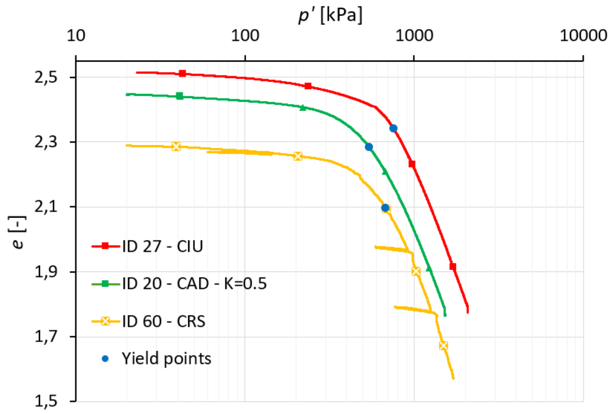

Figure 3. Examples of compression curves.

All compression curves in Figure 3 display a transition from stiff, close to elastic behavior, at lower stresses to post yield compression governed by plastic straining at higher stresses. The yield stress, p'_y, from both the triaxial tests and the CRS tests, is determined from the $p' - e$ curve on a semi-logarithmic scale using the empirical and graphical construction presented by Casagrande (1936). The yield stresses obtained by the Casagrande method were compared with other empirical and graphical approaches, which provided very similar values of the yield stress. Therefore, only the Casagrande-based results are reported. Yield points determined using Casagrande's method generally occurred at the upper boundary of the observed transition zone, suggesting that yielding in cement stabilized gyttja occurs gradually rather than at a distinct stress level. As shown in Table 2, the yield stress tends to decrease as the slope of the consolidation path increases.

Table 3 presents the determined compression parameters, including the slope of the virgin compression line (λ) and the slope of the unloading/reloading paths (κ) in the $p' - e$ curve in semi-logarithmic scale, which are important parameters for modelling soil behavior, as well as the effective strength parameters. The parameters λ and κ are independent of the test type. For the cement stabilized gyttja, λ is determined using the isotropic and anisotropic stress paths from the triaxial tests and from the CRS consolidation tests. The value of κ is only determined based on the CRS consolidation tests, as unloading/reloading was not performed for any of the triaxial tests.

3.2 *Pre- and post-yield shearing behavior*

The general shearing behavior of the cement stabilized gyttja is examined based on the results from the consolidated triaxial tests. Tests are arranged by consolidation state, distinguishing between pre-yield and post-yield conditions.

Figure 4 shows the stress paths in the $p' - q$ space for tests consolidated to a stress level below yielding (pre-yield). An indicative pre-shearing yield surface is shown in Figure 4 based on the yield points found in Table 2 and shown in Figure 6.

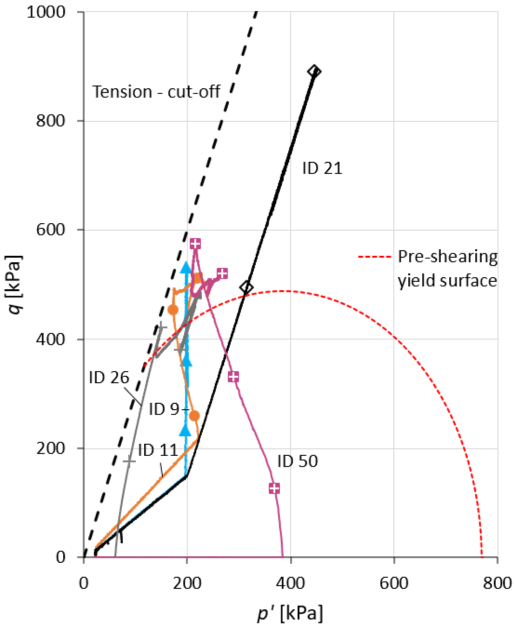

Figure 4. Stress paths – triaxial tests – pre-yield.

An interesting behavior is observed for specimens ID 11, 26, and 50, whose stress paths reach the tension cut-off line. In particular, specimen ID 26 reaches the tension cut-off and follows it until attaining a peak deviatoric stress, after which the stress decreases and subsequently increases again. This indicates the presence of tensile strength and shift in failure mode during straining in the cement stabilized gyttja due to cementation effects. These results show that the shearing behavior of cement stabilized gyttja consolidated at low effective stress levels (pre-yield) is governed by the tension cut-off, which is consistent with previously reported behavior for undrained tests consolidated at low effective stresses (Holdt-Olesen et al., 2025; Åhnberg, 2006).

Figure 5 shows the deviatoric stress, q, and the excess pore water pressure, Δu, against the deviatoric strain, ε_q, for the undrained triaxial test ID 50 (consolidated to pre-yield state). The peak behavior seen in the stress paths is also reflected in the stress-strain curve and pore pressure evolution. Initially, a positive excess pore water pressure is developed indicating that the specimen has a tendency to contract. After the excess pore water pressure reaches its peak, which coincides with the peak in deviatoric stress at a strain level of around 1.5%, the excess pore water pressure reduces slightly, indicating a tendency to dilate.

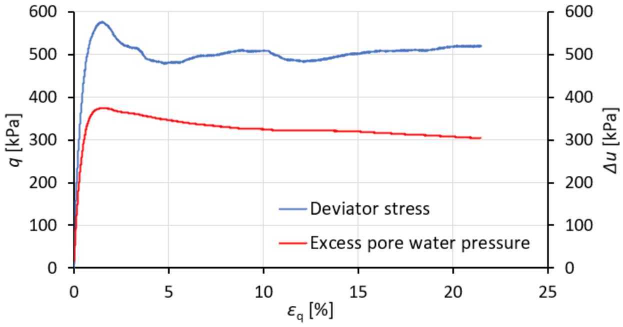

Figure 5. Undrained shearing phase – ID 50 – pre-yield behavior.

The stress paths for the triaxial tests consolidated to a stress level above yield (post-yield) are shown in Figure 6 alongside the initial yield points from the isotropic/anisotropic consolidation phase of the triaxial tests, including the yield points from specimens ID 62 and ID 66, which did not undergo shearing. An indicative pre-shearing yield surface based on the Modified Cam Clay ellipse is approximated using the yield points.

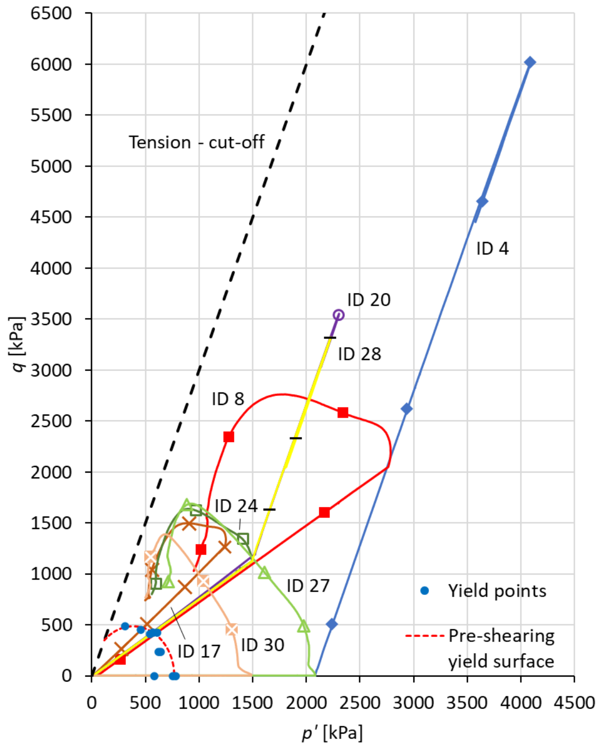

Figure 6. Stress paths – triaxial tests – post-yield.

Figure 6 illustrates that the undrained stress paths of the two isotropically consolidated specimens (ID 27 and ID 30) are nearly identical in shape, indicating that stress level does not significantly influence the shape of the boundary (yield) surface. Similarly, the anisotropically consolidated specimens exhibit comparable undrained stress path geometries; however, their shape differs from that of the isotropically consolidated specimens, suggesting a rotation of the yield surface of the cement stabilized gyttja due to the imposed anisotropic stress condition. An investigation of the detailed yield behavior and the flow rule of the cement stabilized gyttja is beyond the scope of this paper; however, some of these aspects are addressed in Holdt-Olesen et al. (2024).

The deviatoric stress and the excess pore water pressure plotted against the deviatoric strain for the undrained triaxial test ID 8 (consolidated to post-yield state) is presented in Figure 7.

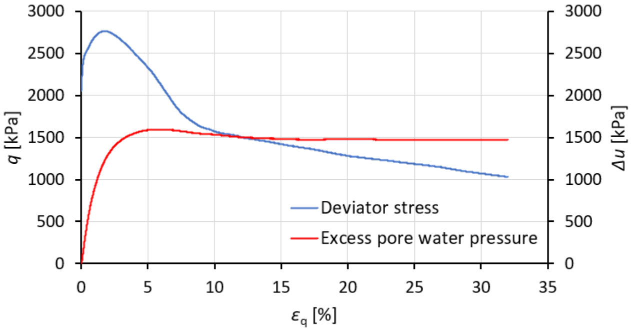

Figure 7. Undrained shearing phase – ID 8 – post-yield behavior.

Specimen ID 8 exhibits very brittle behavior with a distinct peak obtained at low strain level (around 1.8%) and significant softening as is the case for all triaxial tests consolidated to a post-yield stress level. This type of shearing behavior is not typically associated with truly normally consolidated specimens and is explained by cementation effects and breakage of cement bonds. An initial positive excess pore water pressure is developed, indicating a tendency to contract. After a peak excess pore water pressure is reached, the excess pore water pressure remains relatively constant until the end of the test. Unlike the specimen ID 50 (seen in Figure 5), the peak deviatoric stress and the peak excess pore water pressure do not coincide, which is observed in all the post-yield triaxial tests. Both the pre-yield and post-yield triaxial tests exhibit brittle behavior and cementation effects; however, tests consolidated to a post-yield stress state show a greater degree of softening. In all triaxial tests on cement stabilized gyttja, failure occurs along a single shear plane, regardless of whether the shearing phase is drained or undrained. Figure 8 shows examples of the observed failure mechanisms for specimens ID 50 and ID 8.

Figure 8. Failure mechanism. Left: ID 50; right: ID 8.

Previous studies report that axial strain at failure decreases with increasing curing time, curing temperature, and cement content, and that higher strength is often accompanied by a transition from ductile to brittle behavior (Åhnberg, 2006; Holdt-Olesen et al., 2025). In this study, cement content, curing time, and curing temperature were held constant; thus, axial strain at failure is primarily influenced by shearing mode and consolidation stress. Deviatoric strain at failure ranges from 1.2–12.2% in undrained tests; however, most undrained triaxial tests fail at a deviatoric strain in the range of 1.2-3.5%, as seen in Table 2. The deviatoric strain at failure for the drained triaxial tests is in the range of 7.3–19.6%. Several undrained tests reach peak deviatoric stress at very low strains, demonstrating distinctly brittle behavior, whereas drained tests exhibit significantly higher failure strains. This can be explained by the contractant behavior which will lead to lower void ratio in the failure zone in drained test, which will then be reinforced, and hence require further straining to induce complete failure. In contrast, positive excess pore water pressures will further encourage failure in undrained tests as the effective stresses drop in the failure zone.

3.3 *Effective strength parameters*

Effective strength parameters for the cement stabilized gyttja are determined from the performed triaxial tests. The effective friction angle (ϕ') and cohesion (c') were derived from the p'–q plots using the slope (M) and intercept (a) of the failure envelope according to equations (2) and (3), which apply for triaxial compression (Knappet and Craig, 2020).

$$\phi' = \sin^{-1}\left(\frac{3M}{6+M}\right) \tag{2}$$

$$c' = \frac{a(3-\sin(\phi'))}{6\cos(\phi')} \tag{3}$$

The effective strength parameters of the cement stabilized gyttja are determined for both the peak failure points and the final points from the shearing phase of the triaxial tests. In Figure 9, the peak failure points and the final points from the triaxial tests are plotted in the $p'-q$ space. Linear regression is applied to both the peak failure points and the final points in order to determine the effective strength parameters of the cement stabilized gyttja.

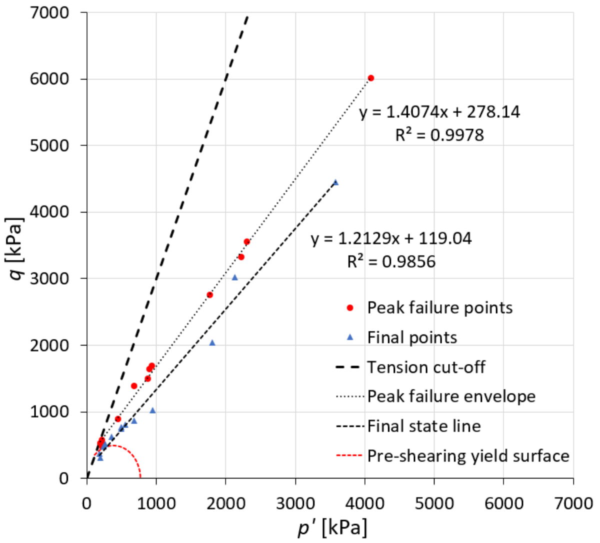

Figure 9. Failure envelopes.

The effective strength parameters determined from the regressions are $\phi'_{\mathrm{p}} = 34.8°$, $c'_{\mathrm{p}} = 137$ kPa for peak conditions, and $\phi'_{\mathrm{fs}} = 30.3°$, $c'_{\mathrm{fs}} = 57$ kPa for the final state. The final state points were also fitted using a linear zero-intercept regression, which produced a good fit with an R^2 value of 0.9803 and a resulting friction angle of 32.5°, consistent with critical state theory. Figure 9 illustrates that both the peak failure envelope and the final state envelope have been determined across a wide stress range and are well represented by linear trends, with no observable curvature at higher (or lower) stress levels. The results show that the peak failure state is characterized by a higher effective friction angle and a greater effective cohesion compared to the final state. As discussed by Lee et al. (2004), the peak strength is primarily controlled by interparticle bonding induced by cementitious materials. Following peak strength, the degradation of these bonds leads to a transition towards a final state where shear resistance is governed primarily by frictional mechanisms along the failure plane.

The final state envelope appears to reflect a convergence towards a common stress condition across the tests. However, due to strain localization and shear band formation, the internal stress distribution within the specimens is uncertain, which affects the reliability of the deviatoric stress and the mean effective stress at larger axial strain levels. This makes it difficult to assess whether a true critical state has been reached at the end of the tests. Although critical state theory predicts zero effective cohesion, the triaxial tests reveal a small effective cohesion in the final state for the cement stabilized gyttja. This can be explained by the fact that even small variations in the dataset may result in a non-zero intercept when fitting a linear trend. Despite these factors, the consistent alignment of the final points suggests that the samples are approaching a similar limiting stress state towards the end of the tests.

To further investigate whether the cement stabilized gyttja approaches a limiting state after peak, the final data points from the shearing phase of the triaxial tests are analyzed in more detail. These points are plotted in a $p' - \nu$ semi-logarithmic scale in Figure 10, where $\nu = 1 + e$ represents the specific volume. Additionally, the initial points and peak failure points are also plotted in Figure 10. The final points are fitted with a straight line in the $p' - \nu$ semi-logarithmic scale.

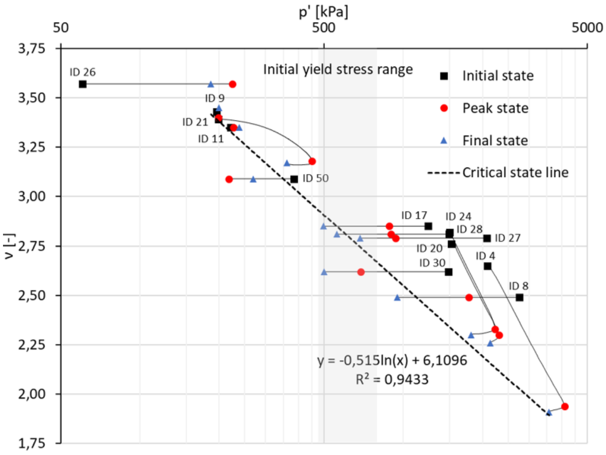

Figure 10. Final state line – semi-log scale (spacing between minor gridlines on the x-axis is $5 \cdot 10^n, n = 1$ to 2).

Figure 10 shows that the final datapoints from the shearing phase of the triaxial tests on the cement stabilized gyttja seem to converge towards a straight line in the $p' - \nu$ semi-logarithmic space. The slope of the final state line in Figure 10 is seen to be in the same range as found for the normal compression line of the cement stabilized gyttja in Table 3.

From Figure 10, it is observed that all specimens in the drained triaxial tests undergo volumetric contraction during shearing. For the post-yield undrained triaxial tests, all specimens exhibit a tendency to contract. Specimens ID 11 and ID 50, which were consolidated to a pre-yield stress level and underwent undrained shearing, show an initial tendency to contract followed by a slight tendency to dilate as also seen in Figure 4. The undrained test ID 26, which was consolidated at a very low effective stress level (pre-yield), exhibits a dilative response during shearing as expected for truly overconsolidated specimens.

4 CONCLUSIONS

The primary objective of this paper is to advance the understanding of the compression and shearing behavior of cement stabilized gyttja, with results not intended for direct practical application. The focus is on characterizing the material response under various stress and loading conditions, including stress levels exceeding those typically encountered in practice. The results provide data for improving constitutive models of cement stabilized soft soils, supporting sustainable ground improvement as an alternative to large-scale soil replacement.

The effects of cementation convert the cement stabilized gyttja from a normally consolidated state to an apparent overconsolidated state by introducing a yield stress that is not representative of the soil's natural stress history. Consolidated triaxial and CRS tests show $\lambda = 0.508 - 0.781$ (avg. 0.610) and $\kappa = 0.025 - 0.037$ (avg. 0.030), with $K_0 \approx 0.38$. Triaxial tests reveal peak strength behavior linked to cementation, with consolidation state influencing dilative or contractive tendencies. Undrained tests fail at lower strains, showing brittle response, while drained tests sustain larger strains before failure.

The effective strength parameters of the cement stabilized gyttja are characterized by higher peak values ($\phi'_p = 34.8°$, $c'_p = 137$ kPa) than final-state values ($\phi'_{fs} = 30.3°$, $c'_{fs} = 57$ kPa), reflecting a transition from cementation-controlled to frictional resistance. The final points from the shearing phase of the triaxial tests seem to reflect a convergence towards a limiting stress state.

As a continuation of this study and the presented results, the authors have also performed tests on remolded cement stabilized gyttja, prepared by breaking down specimens after 28 days of curing, recompacting the soil, and performing triaxial tests and CRS consolidation tests on the remolded material (cf. Holdt-Olesen et al., 2024). Future work will compare the behavior of intact and remolded cement stabilized gyttja to assess the effects of structure and bonding degradation.

5 REFERENCES

Brandt, E.S., Trankjær, H., Mortensen, N., and Sørensen, K.K. 2025. Assessing Undrained Shear Strength in Danish Marine Gyttja: Insights From Field Vane Tests and Plate Load Tests. *19th Nordic Geotechnical Meeting - Göteborg 2024*. Linköping: Svenska Geotekniska Föreningen. Vol. 1, 198-214.

Casagrande, A. 1936. Determination of the preconsolidation load and its practical significance. *Proceedings of the International Conference on SMFE*. Harvard University, Cambridge, MA. Vol III, 60-64.

Helle, T.E. et al. 2021. A new laboratory procedure for preparing soil specimens admixed with binders. *Fjellsprengningsteknikk, Bergmekanik/Geoteknik 2021*. Oslo, Norway, Norsk forening for fjellsprengningsteknikk, Norsk Bergmekanikkgruppe og Norsk Geoteknisk Forening. 45.1-45.15.

Holdt-Olesen, D.F., Holdt-Olesen, N.F., and Jensen, C.O. 2024. *Compression and Shearing Behavior of Cement Stabilized Gyttja*. Master's thesis, Aarhus University.

Holdt-Olesen, D.F., Holdt-Olesen, N.F., Jensen, C.O., Sørensen, K.K., and Lodahl, M.R. 2025. Strength Development and Shearing Behavior of Cement Stabilized Gyttja. *19th Nordic Geotechnical Meeting - Göteborg 2024*. Linköping: Svenska Geotekniska Föreningen. Vol. 2, 363-375.

Janz, M. and Johansson, S.-E. 2002. *The Function of Different Binding Agents in Deep Stabilization - Report 9*. Linkoping: Swedish Deep Stabilization Research Centre.

Kasama, K., Ochiai, H., and Yasufuku, N. 2000. On the Stress-Strain Behaviour of Lightly Cemented Clay Based on an Extended Critical State Concept. *Soils and Foundations*, Vol. 40 (5), 37-47.

Knappet, J. and Craig, R.F. 2020. *Craig's Soil Mechanics*. Ninth Edition. Boca Raton: Taylor & Francis Group.

Larsen, G., Greve, C., and Halkjær, M.W. 2019. Hvornår er det slut med grus i Danmark? *Aktuel Naturvidenskab*, Nr. 4, 12-15.

Lee, K., Chan, D. and Lam, K. 2004. Constitutive Model for Cement Treated Clay in a Critical State Frame Work. *Soils and Foundations*, Vol. 44 (3), 69-77.

Tanderup, M. 2023. *Laboratory Study and Numerical Modeling of Cement Stabilized Aalborg Gyttja*. Master's thesis, Aalborg University.

Åhnberg, H. 2006. *Strength of stabilised soils – A laboratory study on clays and organic soils stabilised with different types of binder*. Doctoral thesis, Lund University.

Åhnberg, H. and Holm, G. 1987. *Om inverkan av härdningstemperaturen på skjuvhållfastheten hos kalk- och cementstabiliserad jord - Report No 30*. Linköping, Swedish Geotechnical Institute.